Med Biol Eng Comput (2010) 48:783–791
DOI 10.1007/s11517-010-0635-9

ORIGINAL ARTICLE

Brain hypothermia induced by cold spinal fluid using a torso cooling pad: theoretical analyses

Katisha D. Smith · Liang Zhu

Received: 27 January 2010 / Accepted: 8 May 2010 / Published online: 4 June 2010

Abstract Brain hypothermia induced by a temperature reduction of the spinal fluid using a torso-cooling pad is evaluated as a cooling alternative for traumatic injury patients. A theoretical model of the human head is developed to include its tissue structures and their contribution to local heat transfer. The Pennes bioheat equation and finite element analysis are used to predict the temperature distribution in the head region. The energy balance in the cerebrospinal fluid (CSF) layer surrounding the brain during mixing of the CSF and cold spinal fluid is also formulated to predict the CSF temperature reduction. Results show that the presence of cooled CSF around the brain provides mild cooling ($\sim$1°C) to the grey matter within 3000 s (50 min) with a cooling capacity of approximately 22 W. However, large temperature variations ($\sim$3.5°C) still occur in the grey matter. This approach is more effective during ischemia because it promotes deeper cooling penetration and results in larger temperature reductions; the average grey matter temperature decreases to 35.4°C. Cooling in the white matter is limited and only occurs under ischemic conditions. The non-invasive nature of the torso-cooling pad and its ability to quickly induce hypothermia to the brain tissue are beneficial to traumatic injury patients.

Keywords Traumatic brain injury · Hypothermia · Cerebrospinal fluid · Ischemia · Temperature

K. D. Smith · L. Zhu (✉)
Department of Mechanical Engineering, University of Maryland, Baltimore County, 1000 Hilltop Circle, Baltimore, MD 21250, USA
e-mail: zliang@umbc.edu

K. D. Smith
e-mail: smithk1@umbc.edu

1 Introduction

Along with the spinal cord, the brain is an essential partner in the central nervous system (CNS), and similarly, it is surrounded and protected from the bony skull and from shock by cerebrospinal fluid (CSF). The brain analyzes information that is both internal and external to the body, transforms the information into sensations, and stores them as memories. Like the spinal cord, the brain is also composed of both grey and white matter, with the grey matter being in direct contact with the CSF. An adult human brain weighs around 3 lbs, which is only about 2% of the total body weight. However, the brain consumes about 20% of the cardiac output.

The brain, like the spinal cord, is also susceptible to permanent neurological damage. Traumatic brain injury (TBI) occurs from external physical trauma, and mostly affects the young population due to motor vehicle accidents [9, 12]. Each year in the United States, about 1.6 million people sustain traumatic brain injuries [12]. Of those incidents, 80,000 result in permanent disability and 52,000 result in death with TBI being the leading cause of death in both North America and Europe [12, 15]. Primary neurological injury to the brain from initial impact trauma includes hematoma, contusion, and axonal injury [11]. Secondary neurological injury does not always immediately follow the moment of impact. It may develop over time following the initial trauma and includes neural cell death, disruption of the blood–brain barrier, increased intracranial pressure (ICP), and ischemia [7–9, 11, 27]. In fact, secondary neurological injury causes the most in-hospital deaths after TBI.

Although the mechanism of neuro-protection from brain hypothermia is still not fully understood, several experimental studies have shown that a temperature reduction of

only 1–2°C in the brain tissue has the potential to preserve brain function, protect against ischemic injury, decrease free radical release, reduce inflammation, and stabilize ICP in the brain [2, 7, 14, 27]. Most clinical studies deal with small subject groups suffering from TBI, and they have shown the protective effects of hypothermia in both the short and long term [4, 15, 16, 22]. One factor that yields a successful outcome following hypothermia treatment is initiating cooling immediately after or prior to injury. Unfortunately, it is not always feasible to reduce the brain temperature before the injury occurs for TBI patients, so developing a cooling method to initiate cooling as soon as possible to TBI patients is desirable.

Since the brain and spinal cord are both integrated into the CNS, it is likely that traumatic injuries affecting the spinal cord, due to car accidents, falls, or sports-related injuries, may also have a negative impact on the brain. Approximately, 50% of traumatic injuries impact both the brain and the spinal cord [28]. Research shows that TBI often occurs with traumatic spinal cord injury (SCI), but TBI is frequently undiagnosed in the presence of SCI and can have a strong negative effect on the total neurological outcome [28]. The feasibility of developing a cooling protocol to decrease the brain and the spinal cord temperatures simultaneously may help provide the most neuroprotection following traumatic injury that afflicts both the brain and the spinal cord.

Our previous theoretical study [31], which simulates the temperature distribution in the spinal cord and its surrounding structures, illustrates the feasibility of reducing the average spinal cord temperature by approximately 2.7°C with the use of a simple cooling pad placed along the back of the human torso. Additionally, this proposed treatment reduces the average global temperature of the spinal fluid surrounding the spinal cord by approximately 3.5°C within 1800 s (30 min). Since the spinal fluid connects with the CSF surrounding the brain hemisphere, brain hypothermia may be possible as the cold spinal fluid constantly replaces part of the warm CSF surrounding the brain hemisphere.

The objective of this study is to evaluate the cooling extent in the brain tissue due to the cold spinal fluid using a torso-cooling pad. We have developed a theoretical model of the human head composed of the scalp, bone, muscle tissue, CSF, and brain tissue. The Pennes bioheat equation [26], in conjunction with finite element analysis (FEA), is used to predict the temperature distribution in the head region. The energy balance in the CSF during the mixing of the fluid surrounding the brain with the spinal fluid is also formulated to predict the temperature reduction in the CSF due to fluid replacement and thermal interaction between the CSF and its surrounding tissue. The coupled equations for the head region and the CSF are solved simultaneously. The simulations predict the extent of temperature reductions in the grey and white matters of the brain based on the temperature of the fluid entering the base of the brain and the temperature of the CSF excreted within the brain. The effect of possible grey matter ischemia following traumatic injury on the temperature reductions is also examined.

2 Mathematical formulation

The mathematical formulation consists of modeling both the head temperature distribution and the energy balance of the CSF layer. The Pennes bioheat equation is used to simulate the tissue temperature field in the head, and a lumped system analysis is used to predict the CSF temperature reduction during the mixing of the cold spinal fluid with the warm CSF surrounding the brain during therapeutic hypothermia using a torso-cooling pad.

2.1 Transient behavior of the spinal fluid temperature

In our previous theoretical simulation [31], the temperature reduction of the fluid surrounding the spinal cord is induced by the use of a cooling pad placed along the back of the torso. The data from that study are used in this current theoretical model to calculate the temperature of the CSF surrounding the brain hemisphere during the cooling process. Cooling from the torso surface penetrates the skin and bony spinal column to the spinal fluid, and after about a half an hour, the temperature of the spinal fluid is reduced by more than 3.5°C. Based on these theoretical simulations, the temperature of the spinal fluid entering the brain cavity is able to establish a steady state within 5400 s (90 min) and a 4.7°C temperature reduction in the spinal fluid entering the brain cavity is achieved. The transient behavior of the average spinal fluid temperature entering the brain cavity is shown in Fig. 1.

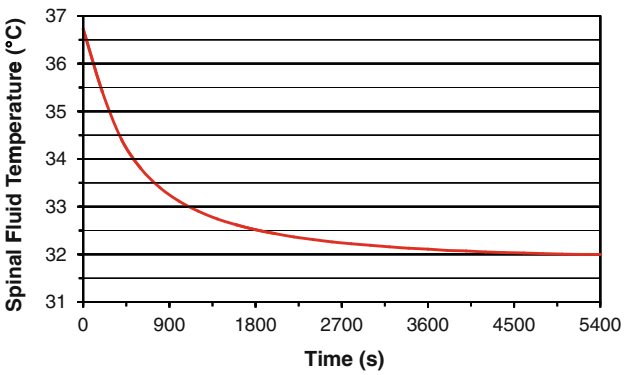

Fig. 1 Transient temperature distribution of spinal fluid at the spinal cavity outlet. It takes 5400 s (90 min) for the fluid temperature to establish a steady state

2.2 Energy balance in the CSF layer

The temperature of the CSF within the brain cavity, T_{csf}, decreases during the torso cooling due to mixing the cold spinal fluid with the CSF surrounding the brain. The CSF also exchanges heat with the surrounding brain and skull tissue structures. In this study, the CSF compartment is modeled as a lumped system where the temperature is a function of time, t, only. The fluid from the spinal region enters the brain cavity during arterial diastole and exits the brain region during arterial systole [31]. Therefore, this study assumes that the total mass of the CSF in the head region is relatively unchanged. The schematic diagram of the CSF layer is illustrated in Fig. 2.

Based on the energy balance of the CSF layer control volume over a small time interval, Δt, the amount of thermal energy that enters the control volume $(\dot{E}_{in})$, plus the amount of thermal energy that is generated within that control volume $(\dot{E}_g)$, minus the amount of thermal energy that leaves the control volume $(\dot{E}_{out})$ must equal the changed amount of energy that is stored within the control volume $(\dot{E}_{st})$. This study assumes that there is no thermal energy generated within the CSF control volume. Therefore, $\dot{E}_{st}$ is represented by:

$$\left(\rho c_p V\right)_{csf} \frac{dT_{csf}}{dt} \tag{1}$$

where ρ is the CSF density (kg/m^3), V is the CSF volume (m^3), and c_p is the CSF specific heat capacity (J/kg K).

Some of the energy that is removed from the control volume is due to replacing a portion of CSF in the brain with the cold fluid entering from the spinal region, which is proportional to the percentage of the CSF being constantly replaced and the temperature difference between the warm CSF and cold spinal fluid. As shown in Fig. 2, energy may also enter the control volume through the CSF-bone (Q_{outer}) and the CSF-brain (Q_{inner}) interfaces by heat conduction. Therefore, the energy conservation equation for the CSF layer in the head can be written as:

$$\begin{aligned}\left(\rho V c_p\right)_{csf} &\frac{T_{csf}(t+\Delta t) - T_{csf}(t)}{\Delta t} \\ &= \left(\rho V c_p\right)_{csf} p_{sp}\left(T_{csf,sp}(t+\Delta t) - T_{csf}(t)\right) \\ &\quad + \left[Q_{outer}(t) + Q_{inner}(t)\right]\end{aligned} \tag{2}$$

The first term on the right side of Eq. 2 represents the energy change due to cold spinal fluid replacing part of the CSF surrounding the brain. $T_{csf,sp}$ is the average temperature of the cold spinal fluid entering the CSF compartment and is given in Fig. 1, and p_{sp} is the percentage of the CSF in the brain that is replaced by the cold spinal fluid per second. Therefore, the first term on the right side provides a cooling capacity (W) by mixing the cold spinal fluid with the CSF surrounding the brain hemisphere. The second term on the right side of Eq. 2 represents the thermal interaction between the CSF and adjacent tissue structures. The heat conduction rate entering the CSF compartment varies as a function of time and the temperature distribution of the tissue structures surrounding the CSF. Therefore, solving Eq. 2 requires determination of the temperature distribution in the head region. The temperature field in the head region will be described in the following section.

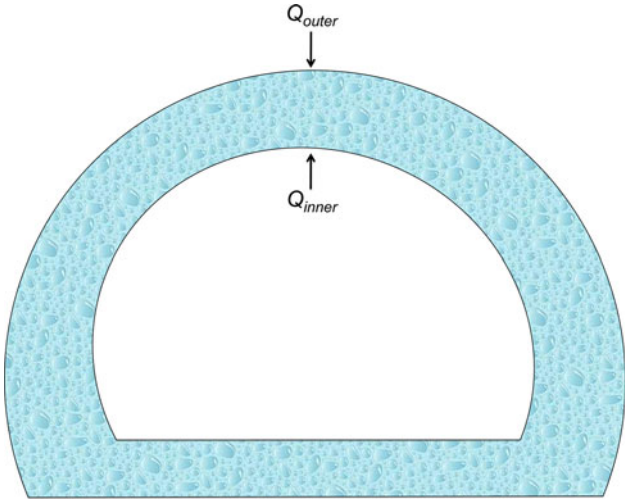

Fig. 2 Schematic diagram of the energy balance in the CSF. The CSF control volume is enlarged and is represented by the *blue color*. Energy can be added to the control volume through both the CSF-brain interfaces (Q_{inner}) and the CSF-skull interfaces (Q_{outer}) by heat conduction

2.3 Theoretical model of the human head

Similar to previous studies [5, 35, 36, 38], the head region is modeled as a three-dimensional structure composed of the grey and white matters, the CSF layer, bone, the scalp and the muscle tissue. The schematic diagram of the head is shown in Fig. 3. The human head is modeled using the continuum approach with the assumption that all the thermal tissue properties are homogeneous and isotropic in individual structures. In this study, the Pennes bioheat equation is used to model the heat transfer in the individual tissue structures and is given by:

$$\begin{aligned}(\rho c)_{wm,gm,bo,sc,m} &\frac{\partial T_{wm,gm,bo,sc,m}}{\partial t} \\ &= k_{wm,gm,bo,sc,m}\nabla^2 T_{wm,gm,bo,sc.m} \\ &\quad + (\rho c)_{bl}\omega_{wm,gm,bo,sc,m}\left(T_a - T_{wm,gm,bo,sc,m}\right) \\ &\quad + q_{mwm,gm,bo,sc,m}\end{aligned} \tag{3}$$

where the subscripts wm, gm, bo, sc, and m refer to the white matter, grey matter, bone, scalp, and muscle, respectively. The second term on the right side of Eq. 3

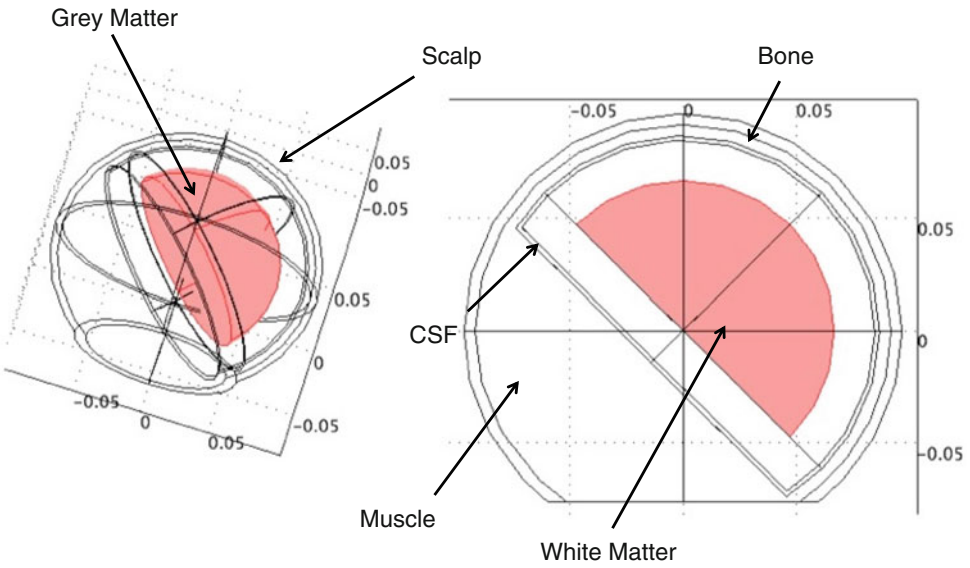

Fig. 3 Three-dimensional schematic diagram (*left*) and cross section (*right*) of head region. The white and grey matters and the CSF are modeled as concentric hemispheres embedded within the bone, scalp, and muscle tissue of the head

describes the thermal contribution due the local blood perfusion rate, ω. The third term on the right side of Eq. 3 represents the volumetric heat generation rate due to the local tissue metabolism. The strength of the volumetric heat generation rate is proportional to the local blood perfusion rate and the temperature difference between the arterial blood, T_a, and the local tissue, T_t. The arterial blood temperature is assumed to equal the core body temperature of 37°C.

For the initial condition, the temperature of the simulated domain is the steady-state temperature prior to cooling. There are three prescribed boundary conditions for the system. The outside head surface is subjected to radiation and natural convection from the surrounding environment ($T_\infty = 25$°C). The overall heat transfer coefficient is calculated as $h = 10.36$ W/m^{2}K ($h_{conv} = 4.17$ W/m^2 K, $h_{rad} = 6.19$ W/m^2 K) [17]. The bottom head surface is assumed adiabatic because of the small heat transfer rate through the bottom surface [35]. The CSF layer is removed from the simulation domain. Therefore, it becomes a boundary condition for the head simulation. The temperature in the CSF, as described by Eq. 2, is modeled as a time-dependent temperature boundary condition, $T_{csf}(t)$, at the interfaces. Therefore, the temperature field of the head region is coupled with the energy balance for the CSF compartment. Both Eqs. 2 and 3 need to be solved simultaneously and are described in the next section.

Temperature distributions in the head region are solved using finite element analysis (FEA). All the finite element calculations and mesh generation are performed using FEMLAB 3.1 (COMSOL, Stockholm, Sweden) on an Apple PowerBook G4 (Mac OS 10.4, 2 GB RAM, 1.67 GHz processor). The Unsymmetric-Pattern Multi-Frontal (UMFPACK) Method with direct LU factorization (0.0001 absolute tolerance and 0.001 relative tolerance) is used to numerically solve Eq. 3. Mesh independency is tested by doubling the number of mesh elements from the initial mesh of approximately 90,000 elements. The finer mesh (186,400 elements) provides a less than 1% difference in the average global temperature in the CSF and the grey and white matters. The final volumetric mesh for the simulated domain contains 186,400 tetrahedral Lagrange linear elements.

2.4 Procedures for solving coupled equations

The governing equation for the CSF temperature and the Pennes bioheat equation for the head region are coupled. This section provides the procedures used to simultaneously solve both equations. Equation 2 is first discretized over a finite time interval, Δt, using the explicit scheme of the finite difference method as follows:

$$(\rho V c_p)_{csf} \frac{T_{csf}^{P+1} - T_{csf}^{P}}{\Delta t} = (\rho V c_p)_{csf} p_{sp} \left(T_{csf,sp}^{P} - T_{csf}^{P} \right) + Q_{outer}^{P} + Q_{inner}^{P} \quad (4)$$

where superscripts P and $P + 1$ represent the previous and current time instants, respectively, T_{csf}^{P+1} is the temperature of the CSF within the brain cavity at time, $t + \Delta t$. T_{csf}^{P} is the average temperature of the CSF within the brain cavity at time, t. Microsoft Excel is used to calculate T_{csf} at each time step (Eq. 4). The following general procedures are used to solve Eqs. 3 and 4 simultaneously:

(1) Use FEMLAB to solve for the steady state temperature field of the head region before cooling is initiated. The steady state temperature field serves as the initial temperature field for the transient analysis

($P = 0$). For $P = 0$, the summation of Q_{inner} and Q_{outer} should equal zero because of the original steady state condition.

(2) Substitute the spinal fluid temperature (T) as determined from Fig. 1 and the summation of Q_{inner} and Q_{outer} into Eq. 4 and calculate the CSF temperature for the next time instant $\left(T_{\text{csf}}^{1}\right)$.

(3) Input the newly calculated value $\left(T_{\text{csf}}^{P+1}\right)$ into the Pennes bioheat equation as the CSF boundary condition into the FEMLAB software and solve for the transient temperature distribution of the head region over a time duration, Δt.

(4) Calculate the values of Q_{inner} and Q_{outer} at the end of the time duration, Δt, during postprocessing in the FEMLAB software by multiplying the total surface area of the inner and outer surfaces with their respective total normal conductive heat fluxes. Both the values of Q_{inner} and Q_{outer} and $T_{\text{csf,sp}}$ from Fig. 1 are then substituted into Eq. 4 to calculate T_{csf} for the next time step.

(5) Repeat Steps 3 and 4 to solve for the transient temperature fields for the subsequent time steps.

Since the accuracy of the explicit scheme depends on the time step, Δt, in the study, the sensitivity of the simulation on the time step is evaluated to determine how temperature distribution is affected by the time step. Initially, the time step is selected as 10 min. Then, it is subsequently decreased by 50% until the change in the time step results in a less than 1% difference in the simulated temperature field. The final time step is 30 s, and the total simulation time is 5400 s (90 min).

3 Results

The physical, geometrical, and physiological parameters under normal conditions used in the proposed model are provided by previous studies [5, 13, 20, 21, 25, 35, 36] and are listed in Table 1. The head is modeled as a partial sphere with a radius of 97 mm. The CSF compartment is 2 mm thick. The brain, which consists of grey and white matter, is modeled as a hemisphere with an 85 mm radius. Similar to the spinal cord, the brain also has high metabolic and blood perfusion rates; the perfusion and metabolic rates for the grey matter are four times that of the white matter. During normal and ischemic conditions, the local blood perfusion rate in each tissue structure is assumed to be proportional to the local metabolic heat generation rate. From the literature [23, 24, 29–31], the average amount of CSF in the body is 137.5 ml and 37% (50.88 ml) of that amount fills the brain cavity when the body is in a horizontal position. Based on previous theoretical results [23, 31], the volume of cold spinal fluid replacing the CSF in the brain cavity during a pulsatile cycle with a 1-s period is calculated as 4.28 ml. From this, the percentage of warm CSF in the brain that is replaced by cold spinal fluid per second, p_{sp}, in Eq. 4 is calculated as 8.4% per second.

Figure 4 shows the average transient temperature profiles for the spinal fluid entering the brain ($T_{\text{csf,sp}}$), the CSF surrounding the brain (T_{csf}), the grey matter (T_{gm}), and the white matter (T_{wm}) during 5400 s (90 min) of cooling using the proposed non-invasive hypothermia method. The decrease in the average spinal fluid is 4.73°C, and there is a reduction of 3.68°C in the average temperature of the CSF surrounding the brain. Cooling decreases the average grey matter temperature by approximately 1°C, and it appears that the grey brain matter establishes a steady state within 3000 s (50 min). For this study, the characteristic time, t_{c}, needed to reach a steady state during the transient process is defined as

$$\frac{T(t_{\text{c}}) - T(0)}{T_{\text{c}} - T(0)} = 99\% \tag{5}$$

where $T(0)$ is the initial temperature and T_{c} is the steady state temperature. However, the brain white matter temperature ($\sim$37.14°C) remains almost unchanged during the entire cooling protocol. The temperature contours of the

Table 1 Physical, geometrical, and physiological parameters under normal conditions

Parameter	Specific heat capacity, c (J/kg K)	Density, ρ (kg/m^3)	Thermal conductivity, k (W/mK)	Blood perfusion rate, ω (1/s)	Metabolic heat generation rate, q_{m} (W/m^3)	Radius, R (mm)
Blood	3800[a]	1050[a]	–	–	–	–
Muscle	3700[f]	1050[f]	0.5[f]	0.000167[f]	180.2[f]	–
Scalp	4000[a]	1000[a]	0.34[a]	3.34e-4[a]	363.4[a]	97[a]
Bone	2300[a]	1500[a]	1.12[a]	3e-4[a]	368.3[a]	92[a]
CSF	4178.3[b]	1000.3[b]	0.623[b]	–	–	87[c,d,e,g]
Grey Matter	3700[a]	1050[a]	0.5[a]	0.01333[a]	16700[a]	85[a]
White Matter	3700[a]	1050[a]	0.5[a]	0.00333[a]	4175[a]	67[a]

[a] [5], [b][13], [c][20], [d][21], [e][25], [f][35], [g][36]

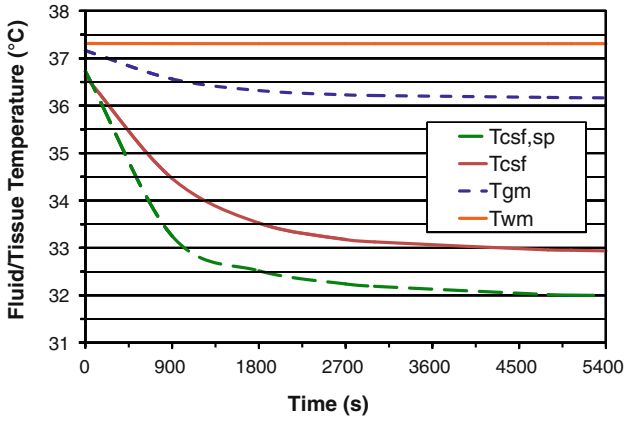

Fig. 4 Average transient temperature profiles of the spinal fluid ($T_{csf,sp}$), the CSF in the brain cavity (T_{csf}), the grey matter (T_{gm}), and the white matter (T_{wm}) during 5400 s (90 min) of cooling

human head region before and after cooling are shown in Fig. 5. The brain temperature at the outermost layer is 33.57°C, and temperature continues to increase toward the deeper regions of the brain matter. From the figure, one can see that cooling to the brain is limited to the superficial layers of the grey matter, and cooling is unable to reach the white matter. Figure 6 illustrates the cooling penetration through the brain matter along line A–B in Fig. 5 before cooling and after cooling during normal and ischemic conditions. The maximum brain temperature prior to cooling is slightly higher than the arterial blood temperature of 37°C due to its high metabolic heat generation rate. Cooling in the CSF results in significant temperature reductions in the grey matter. The data show that cooling penetration is limited to the peripheral region in the grey matter, and the white matter temperature remains constant during the cooling process.

Table 2 provides the calculated values of Q_{inner} and Q_{outer} during the cooling process. Although the table only shows these values for every 450 s (7.5 min), Q_{inner} and Q_{outer} are calculated every 30 s in the simulation. Initially, the summation of these two values is zero due to the initial steady state. A negative value of the heat transfer rate, Q, from the CSF layer surface implies that heat is released from the CSF layer to the surrounding tissue, while a positive value for Q implies that heat is added to the CSF layer from the surrounding tissue environment. As the temperature of the CSF surrounding the brain continues to decrease due to the cold spinal fluid entering the system, both the values of Q_{inner} and Q_{outer} become positive as more heat from the surrounding tissue is added to the CSF layer. It is also shown that the heat from the brain tissue to the CSF layer (Q_{inner}) is larger than the heat from the bone to the CSF layer (Q_{outer}) due to the higher temperatures inside the brain tissue than that in the bone tissue. As temperatures reach a steady state after 3000 s of cooling, both Q_{inner} and Q_{outer} stabilize to approximately 0.3 and 22 W, respectively, and balance the cooling capacity induced by the cold spinal fluid.

A simple parametric study is conducted to test the effect of grey matter ischemia on the temperature distribution of both the grey and white brain matters, since the grey matter is more susceptible to ischemia than the white matter [5]. The local blood perfusion and volumetric heat generation rates in the grey matter are reduced to 20% of their normal

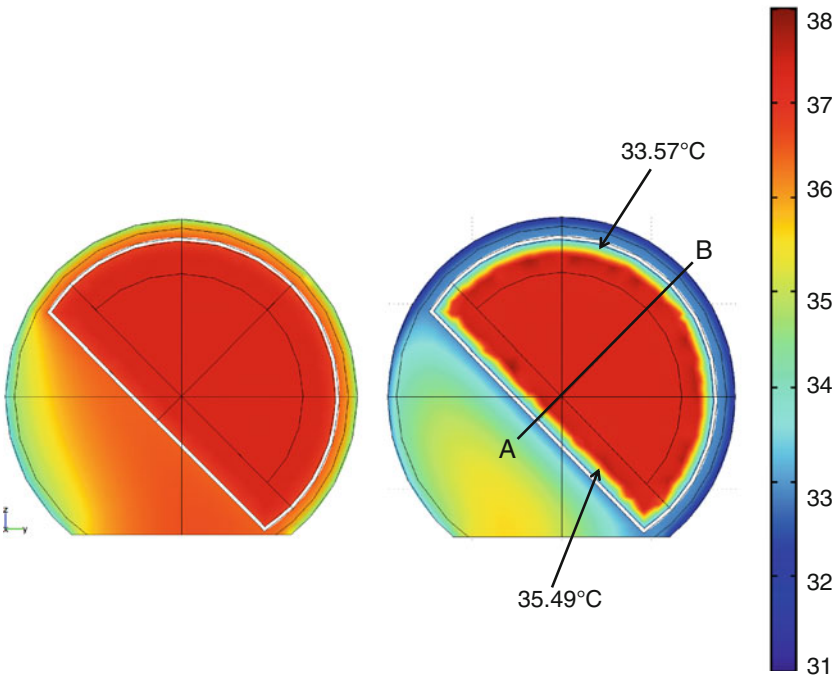

Fig. 5 Temperature contours of the head region before cooling at $t = 0$ s (*left*) and after cooling at $t = 5400$ s (*right*)

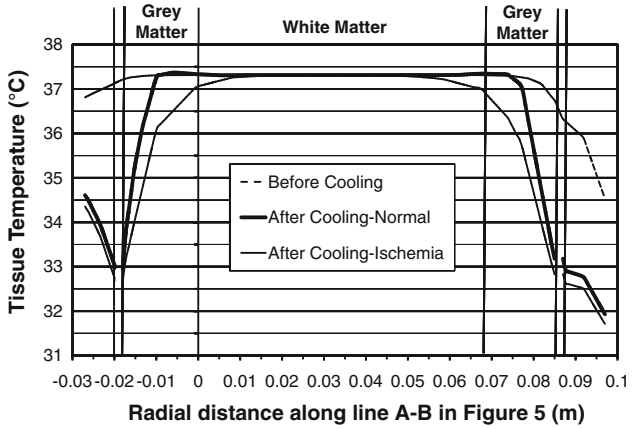

Fig. 6 Radial temperature distribution in the brain tissue along line A–B, as shown in Fig. 5, before cooling (*dashed line*) and after cooling for normal (*heavy solid line*) and grey matter ischemic (*solid line*) conditions

Table 2 Calculated values of Q_{inner} and Q_{outer} during the cooling process

Time (s)	Q_{outer} (W)	Q_{inner} (W)
0	−2.815828	2.815828
450	−0.661394	9.089275
900	0.899108	14.443219
1350	0.800758	17.490906
1800	0.569807	19.211515
2250	0.412996	20.237975
2700	0.352563	20.973807
3150	0.360061	21.332204
3600	0.31921	21.595816
4050	0.243145	21.832124
4500	0.213226	22.001099
4950	0.270896	22.101844
5400	0.298178	21.523244

values because the rates have a coupled relationship. The blood perfusion rate under normal conditions, $\omega_{gm} = 0.01333\ s^{-1}$ (80 ml min^{-1}100 g^{-1}), is reduced to the ischemic value, $\omega_{gm} = 0.00267\ s^{-1}$ (16 ml min^{-1} 100 g^{-1}), and the local metabolic heat generation rate is reduced from 16700 to 3340 W/m^3. Figure 7 compares the average global transient temperature distributions of the grey and white matters under normal and ischemic conditions. The red and blue lines represent the temperatures of the white and grey matters, respectively. Grey matter ischemia increases the temperature reduction of T_{gm} by 84% from 1°C under normal conditions to 1.84°C during grey matter ischemia. Although ischemia is not present in the white matter, grey matter ischemia provides a slight temperature reduction of 0.15°C in the white matter. The presence of ischemia also changes the characteristic time needed for the grey matter temperature to establish a steady state. Under normal conditions, the grey matter temperature reaches a steady state within 3000 s (50 min) of cooling. During ischemia, the characteristic time needed for the grey matter temperature to a reach steady state increases to 5040 s (84 min). As shown in Fig. 6, the temperature profile along line A–B in Fig. 5 also illustrates the radial temperature variation in the brain hemisphere during brain ischemia. Most of the temperature reduction in the grey matter occurs close to the CSF–grey matter interface, and limited cooling in the brain white matter can be seen in the superficial region due to the cooling penetration from the brain grey matter. For this study, cooling penetration is defined as tissue that has achieved at least a 1°C temperature reduction from the baseline temperature of 37.31°C along the line A–B. Under normal conditions, the cooling penetration depth is approximately 5 mm from the CSF–grey matter interface. Grey matter ischemia more than doubles the cooling penetration depth to 13 mm.

4 Discussion

Several methods for inducing selective hypothermia within brain tissue have been proposed and implemented, which include epidural cooling, cooling helmet, nasopharyngeal cooling, forced convection using a fan, and cooling the blood supplied to the brain [1, 3, 6, 10, 18, 19, 22, 34]. These experimental studies show positive neuroprotection of hypothermia in preventing permanent damage by decreasing the brain temperature by up to 7°C within an hour. However, the methods that result in the biggest temperature reductions within a short duration are the more invasive methods that may involve surgical intervention and patient discomfort, such as epidural cooling, direct cooling of the brain blood supply, and nasopharyngeal cooling [1, 3, 10, 35].

In this study, the temperature of the brain during a proposed non-invasive spinal cord hypothermia treatment session is simulated. The results of the study show that under normal conditions, a cooling capacity of approximately 22 W occurs due to the cold spinal fluid that mixes with the warm CSF surrounding the brain hemisphere using a torso-cooling pad. It has been predicted that mild hypothermia (~36°C) may be achievable within 50 min in the grey matter; the white matter temperature remains relatively unchanged. These results are in agreement with several previous theoretical studies [5, 25, 32, 33, 38], which all report that most cooling occurs in the outermost layers of the brain region when surface cooling is implemented. Also, previous theoretical studies have shown that the reduced blood perfusion and the metabolic heat generation rates associated with ischemia allow for deep

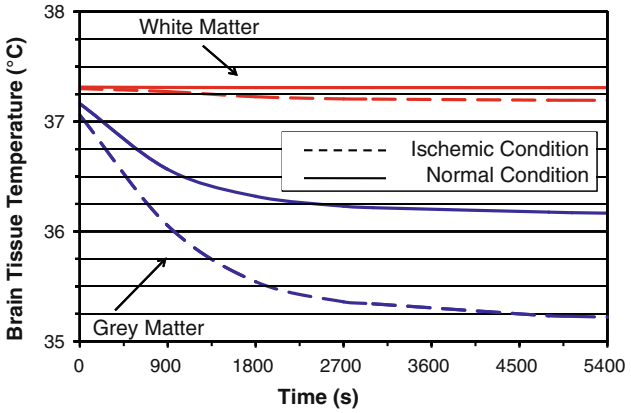

Fig. 7 Transient temperature distributions of the grey (*blue*) and white (*red*) matters under normal (*solid line*) and grey matter ischemic (*dashed line*) conditions

cooling in the affected region [5, 38, 39]. The presence of ischemic injury provides 84% more temperature reduction in the grey matter, 1.84°C during ischemia and 1.0°C under normal conditions. The strength of the blood perfusion rate in brain tissue affects both the achievable cooling penetration and the characteristic time necessary to reach a steady state. A smaller blood perfusion rate increases the cooling penetration to the brain tissue. However, it takes longer for the brain temperature to establish a steady state [5].

The CSF within the subarachnoid space of the brain can be seen as a possible heat exchanger between the brain and its surrounding environment [37]. The mixture of the cold CSF from the spinal cavity and the warm CSF excreted from the brain cavity provides up to 13 mm of cooling penetration to the brain tissue. This means that the use of the proposed cooling pad for reducing the spinal cord temperature has a secondary benefit of inducing hypothermia within the brain tissue, especially in the superficial layers of the grey matter.

Limitations associated with this study are based on the simplified geometry of the head region and the implementation of the Pennes bioheat equation. The shape of the brain is not exactly hemispherical. However, the assumed volume of the brain is based on average brain dimensions and provides a reasonable prediction of the average brain temperature. Since the Pennes equation is a continuum model, it is not possible to solve for point-to-point temperature variations with the results of this study. However, using the Pennes continuum approach is beneficial, since the main interest of this study is to find how cooling affects an entire control volume. The current model based on simple brain geometry provides a reasonable prediction of the temperature distribution in the brain tissue during the proposed cooling protocol.

5 Conclusions

The Pennes bioheat equation and finite element analysis are used to simulate the temperature distribution in the head region during therapeutic hypothermia using a torso-cooling pad for 5400 s (90 min). The results from the theoretical simulation show that the presence of cold CSF from the spinal cavity provides a mild decrease in the grey matter temperature with the most significant cooling occurring in the superficial layers and has no significant effect on the white matter temperature. However, the presence of ischemia in the grey matter increases cooling extent to the brain. The ability to cool the brain tissue during hypothermia treatment for traumatic SCI may become especially beneficial, since traumatic spinal cord injuries often inadvertently promote ischemic injury in the brain for patients also suffering from TBI.

Acknowledgements This research was supported in part by the State of Maryland TEDCO fund, an NIGMS Initiative for Minority Student Development Grant (R25-GM55036), and Procter and Gamble. This research was performed in partial fulfillment of the requirements for the Ph.D. degree from the University of Maryland, Baltimore County by Katisha D. Smith.

References

1. Allers M, Boris-Möller F, Lunderquist A et al (2006) A new method of selective, rapid cooling of the brain: an experimental study. Cardiovasc Interv Rad 29:260–263
2. Busto R, Dietrich W, Globus M et al (1989) The importance of brain temperature in cerebral ischemic injury. Stroke 20:1113–1114
3. Cheng H, Shi J, Zhang L et al (2006) Epidural cooling for selective brain hypothermia in porcine model. Acta Neurochir 148:559–564
4. Davies A (2005) Hypothermia improves outcome from traumatic brain injury. Crit Care Resusc 7:238–243
5. Diao C, Zhu L, Wang H (2003) Cooling and rewarming for brain ischemia or injury: theoretical analysis. Ann Biomed Eng 31:346–353
6. Diao C, Zhu L (2006) Temperature distribution and blood perfusion response in rat brain during selective brain cooling. Med Phys 33:2565–2573
7. Dietrich W (1992) The importance of brain temperature in cerebral injury. J Neurotraum 9:S475–S485
8. Dietrich W, Atkins C, Bramlett H (2009) Protection in animal models of brain and spinal cord injury with mild to moderate hypothermia. J Neurotraum 26:301–312
9. Diller K, Zhu L (2009) Hypothermia therapy for brain injury. Annu Rev Biomed Eng 11:135–162
10. Dohi K, Jimbo H, Abe T et al (2006) Positive selective brain cooling method: a novel, simple, and selective nasopharyngeal brain cooling method. Acta Neurochir 96:406–412
11. Fu E, Tummala R (2005) Neuroprotection in brain and spinal cord trauma. Curr Opin Anaesthesiol 18:181–187
12. Ghajar J (2000) Traumatic brain injury. Lancet 356:923–929
13. Goetz T, Romero-Sierra C, Ethier R et al (1988) Modeling of therapeutic dialysis of cerebrospinal fluid by epidural cooling in spinal cord injuries. J Neurotraum 5:139–150

14. Gupta A, Al-Rawi P, Hutchinson P et al (2002) Effect of hypothermia on brain tissue oxygenation in patients with sever head injury. Br J Anaesth 88:188–192
15. Henderson W, Dhingra V, Chittock D et al (2003) Hypothermia in the management of traumatic brain injury: a systematic review and meta-analysis. Intensive Care Med 29:1637–1644
16. Hutchinson J, Ward R, Lacroix J, Hebert P, Barnes M, Bohn D, Dirks P, Doucette S, Fergusson D, Gottesman R, Joffe A, Kirpalani H, Meyer P, Morris K, Moher D, Singh R, Skippen P (2008) Hypothermia therapy after traumatic brain injury in children. New Engl J Med 358:2447–2456
17. Incropera F, DeWitt D (1996) Fundamentals of heat and mass transfer, 4th edn. Wiley, New York
18. Kuluz J, Prado R, Chang J et al (1993) Selective brain cooling increases cortical cerebral blood flow in rats. Am J Physiol 265:H824–H827
19. Laptook A, Shalak L, Corbett R (2001) Differences in brain temperature and cerebral blood flow during selective head versus whole-body cooling. Pediatrics 108:1103–1110
20. Linninger A, Tsakiris C, Zhu D et al (2005) Pulsatile cerebrospinal fluid dynamics in the human brain. IEEE Trans Biomed Eng 52:557–565
21. Linninger A, Xenos M, Zhu D et al (2007) Cerebrospinal fluid flow in the normal and hydrocephalic human brain. IEEE Trans Biomed Eng 54:291–302
22. Liu W, Qiu W, Zhang Y et al (2006) Effects of selective brain cooling in patients with severe traumatic brain injury: a preliminary study. J Int Med Res 34:58–64
23. Loth F, Yardimmci M, Alperin N (2001) Hydrodynamic modeling of cerebrospinal fluid motion within the spinal cavity. J Biomech Eng 123:71–79
24. Magnæs B (1989) Clinical studies of cranial and spinal compliance and the craniospinal flow of cerebrospinal fluid. Br J Neurosurg 3:659–668
25. Nelson D, Nunneley S (1998) Brain temperature and limits on transcranial cooling in humans: quantitative modeling results. Eur J Appl Physiol 78:353–359
26. Pennes H (1948) Analysis of tissue and arterial blood temperatures in the resting human forearm. J Appl Physiol 1:93–122
27. Polderman K (2004) Application of therapeutic hypothermia in the ICU: opportunities and pitfalls of a promising treatment modality. Part 1: indications and evidence. Intensive Care Med 30:556–575
28. Povolny M, Kaplan S (1993) Traumatic brain injury occurring with spinal cord injury: significance in rehabilitation. J Rehabil 59:1–8
29. Saunders N, Habgood M, Dziegielewska K (1999) Barrier mechanisms in the brain. Clin Exp Pharmacol Physiol 26:11–19
30. Schellinger D, LeBihan S, Rajan S et al (1992) MR of slow CSF flow in the spine. Am J Neuroradiol 13:1393–1403
31. Smith K, Zhu L (2010) Theoretical evaluation of a simple cooling pad for inducing hypothermia in the spinal cord following traumatic injury. Med Biol Eng Comput 48:167–175
32. Sukstanskii A, Yablonskiy D (2004) An analytical model of temperature regulation in human head. J Therm Biol 29:583–587
33. Van Leeuwen G, Hand J, Lagenduk J et al (2000) Numerical modeling of temperature distributions within the neonatal head. Pediatr Res 48:331–356
34. Wang H, Olivero W, Lanzion G et al (2004) Rapid and selective cerebral hypothermia achieved using a cooling helmet. J Neurosurg 100:272–277
35. Wang Y, Zhu L (2007) Targeted brain hypothermia induced by an interstitial cooling device in human neck: theoretical analyses. Eur J Appl Physiol 101:31–40
36. Xu X, Tikusis P, Giesbrecht G (1999) A mathematical model for human brain cooling during cold-water near-drowning. J Appl Physiol 86:265–272
37. Zenker W, Kubik S (1996) Brain cooling in humans—anatomical considerations. Anat Embryol 193:1–13
38. Zhu L, Diao C (2001) Theoretical simulation of temperature distribution in the brain during mild hypothermia treatment for brain injury. Med Biol Eng Comput 39:681–687
39. Zhu L, Rosengart A (2008) Cooling penetration into normal and injured brain via intraparenchymal brain cooling probe: theoretical analyses. Heat Transfer Eng 29:284–294